




Adaptive digital predistortion based on Feedback–Wiener Model for aeronautical applications

Tayeb H. C. Bouazza¹ , Smail Bachir¹, Matthieu Pastore² and Claude Duvanaud¹

¹XLIM Laboratory, UMR CNRS 7252, University of Poitiers and ²TELERAD Society, Anglet, France

Research Paper

Cite this article: Bouazza THC, Bachir S, Pastore M, Duvanaud C (2023). Adaptive digital predistortion based on Feedback–Wiener Model for aeronautical applications. *International Journal of Microwave and Wireless Technologies* **15**, 1635–1642. <https://doi.org/10.1017/S1759078723000491>

Received: 14 January 2023

Revised: 5 April 2023

Accepted: 5 April 2023

Keywords:

adaptive linearization; digital predistortion; Feedback–Wiener model; parameter estimation

Corresponding author:

Tayeb H. C. Bouazza,

E-mail:

tayeb.habib.chawki.bouazza@univ-poitiers.fr

Abstract

In this work, a new adaptive digital predistorter (DPD) is proposed to linearize radio frequency power amplifiers (PA). The DPD structure is composed of two sub-models. A Feedback–Wiener sub-model, describing the main inverse nonlinearities of the PA, combined with a second sub-model based on a memory polynomial (MP) model. The interest of this structure is that only the MP model is identified in real time to compensate deviations from the initial behavior and thus further improve the linearization. The identification architecture combines offline measurement and online parameter estimation with small number of coefficients in the MP sub-model to track the changes in the PA characteristics. The proposed structure is used to linearize a class AB 75 W PA, designed by Telerad society for aeronautical communications in Ultra High Frequency (UHF) / Very High Frequency (VHF) bands. The obtained results, in terms of identification of optimal DPD and the performances of the digital processing, show a good trade-off between linearization performances and computational complexity.

Introduction

Aeronautical communications cover critical areas such as aircraft–ground, aircraft–aircraft, and aircraft–satellite links. Due to the transmission of critical data such as voice exchanges, physical/safety parameter measurements, speed, and position, it is important to ensure the efficiency and the robustness of the radio link. Another constraint is the spectrum saturation of the Ultra High Frequency (UHF) and Very High Frequency (VHF) bands due to the requirements of high data rate, network capacity, and the increasing number of connected aircrafts with the continuous growth in global traffic [1, 2]. Spectral congestion imposes RF protocols with strong frequency criteria on the in-band and out-band of the transmitted signals. For example, the VDL2 (VHF DataLink for aircraft and ground stations) requires an Error Vector Magnitude (EVM) less than 6% and an Adjacent Channel Power Ratio (ACPR) of -65 dBc to -85 dBc according to the band.

In this context, power amplifiers (PA) are critical elements of the transmitter system in aircraft communications in terms of energy and linearity. The use of new modulation schemes to increase spectral efficiency and data rates leads to strong envelope variations that make the signal sensitive to PA nonlinear characteristics [3–6]. These nonlinearities generate distortions in the signal band and cause spectral regrowths in the adjacent channels, considered as disturbances for the other users [7, 8]. To reduce these effects, PAs are often oversized for use at a certain Back-Off from their maximum power, thus limiting their power efficiency [9]. Unfortunately, a good efficiency is obtained at the price of poor linearity, especially with modern communication waveforms with high envelope fluctuations and large bandwidths.

In order to reduce this Back-Off while maintaining good transmission quality, linearization techniques [10–15], such as digital predistortion, have proven to be effective and are widely used in numerous wireless communication systems [16–20]. Their principle is to digitally predistort the complex signal envelope in order to compensate the PA distortions [21, 22]. Therefore, complex mathematical functions are implemented to describe its gain/phase inverse characteristics and memory effects. In the literature, various models are used as a predistorter, such as the Volterra series and their variations like Hammerstein or Wiener models [23–27], the Memory Polynomial (MP) model [28, 29], the Generalized Memory Polynomial (GMP) model [30–32], or the cascaded models [33, 34]. In these models, a large number of coefficients is required to achieve good accuracy, but this has the consequence of making their implementation complex and slowing down the estimation process, especially when considering the real-time linearization.

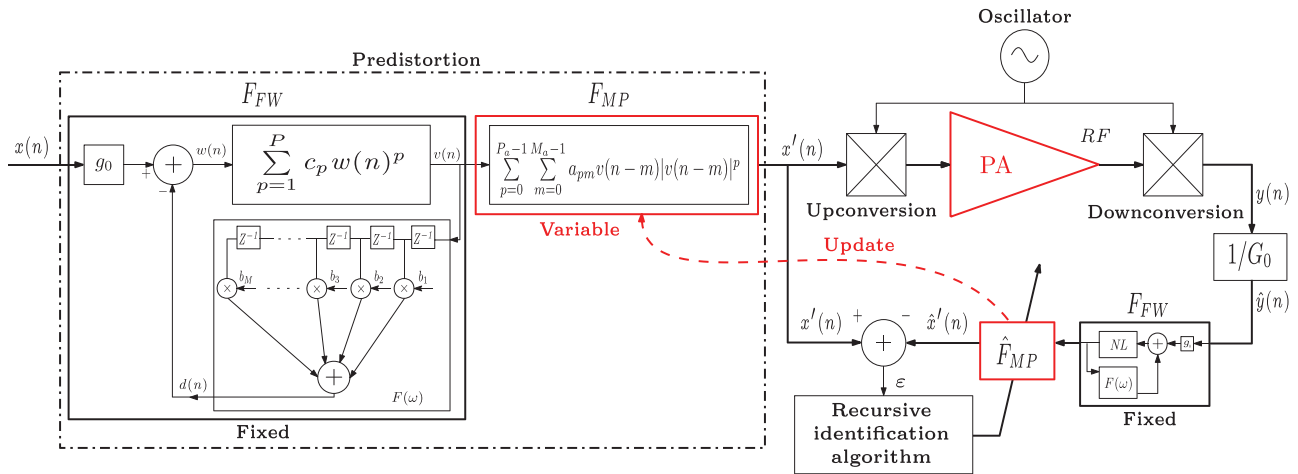


Figure 1. Online DPD based on the FWMP model.

In this work, we propose to study the FWMP model (for *Feedback-Wiener with Memory Polynomial*) as a complexity-reduced predistortion function [35]. The architecture is derived from the study of the electrical constitution of an amplifier. It includes an FW model, which is optimized to characterize the main inverse behavior of the PA and then kept unchanged. A second block MP, optimized in real time, then comes to model the operating deviations with regards to the initial inverse characteristic. A block-oriented DPD function using this structure has been tested for the linearization in real time of a 75 W PA devoted to UHF/VHF for aircraft-ground links.

This paper is organized as follows. In section “Online DPD based on the FWMP model,” we introduce the proposed adaptive linearization architecture, based on a Feedback–Wiener (FW) system. The results of the identification of the optimal DPD structure, the linearization performances using the proposed structure through experimental tests, and a comparison with the MP model are presented in section “Experimental results.” Finally, conclusions are given in the last section.

Online DPD based on the FWMP model

The proposed adaptive linearization architecture is illustrated in Fig. 1. It is based on an Indirect Learning Architecture [36, 37] for updating the coefficients of the MP block [35].

Predistorter structure

As shown in Fig. 1, the proposed DPD structure is based on a combination of two blocks: a FW system that models the main behavior, that is, the interaction between nonlinearities and memory effects, and an MP model to compensate the remaining modeling errors [38]. The FW block itself is composed of two sub-blocks: a memoryless nonlinearity in the direct path and a finite impulse response (FIR) filter in the feedback path, where z^{-1} is the unit delay.

Each block of the DPD is described using the equivalent complex envelope model. The output $v(n)$ of the FW system is given by the following polynomial expression:

$$v(n) = \sum_{p=1}^P c_p \cdot w(n)^p = \sum_{p=1}^P c_p \cdot (g_0 \cdot x(n) - d(n))^p, \quad (1)$$

where c_p are the complex coefficients of the nonlinear function, g_0 is a complex gain, and P is the nonlinearity order. $x(n)$ is the complex envelope of the input signal.

The feedback block $F(\omega)$ is implemented by an FIR filter, and its output $d(n)$ can be formulated as

$$d(n) = \sum_{m=1}^M b_m \cdot v(n - m), \quad (2)$$

where M is the memory depth of the FIR filter.

The signal $v(n)$ is used as an input to the MP model [8]:

$$x'(n) = \sum_{p=0}^{P_a-1} \sum_{m=0}^{M_a-1} a_{pm} \cdot v(n - m) \cdot |v(n - m)|^p, \quad (3)$$

where $x'(n)$ is the predistorted signal, P_a and M_a are the nonlinearity order and the memory depth, respectively.

A great advantage of the MP model in the identification is that it is linear in parameters, allowing a least squares (LS) algorithm. We can introduce its regression form, where $\hat{\theta}_{MP}$ is the vector of parameters to be estimated and $\phi(n)$ is the regressor vector, such that

$$\hat{x}'(n) = \phi(n)^T \cdot \hat{\theta}_{MP}, \quad (4)$$

with

$$\begin{aligned} \hat{\theta}_{MP} &= [a_{00} \cdots a_{p_m} \cdots a_{(P_a-1)(M_a-1)}]^T \\ \phi(n) &= [\phi_{00}(n) \cdots \phi_{p_m}(n) \cdots \phi_{(P_a-1)(M_a-1)}(n)]^T \end{aligned} \quad (5)$$

such as the regressor elements are

$$\phi_{p_m}(n) = |v(n - m)|^{p-1} \cdot v(n - m) \quad (6)$$

Note that, since nonlinearities and memory effects are treated separately in the FW block, the proposed model has the advantage of having an additive evolution in the number of its first block coefficients, unlike the GMP model [30]. Therefore, the total number of coefficients is given by

$$N_{FWMP} = \overbrace{(P + M)}^{FW} + \overbrace{(P_a \times M_a)}^{MP}. \quad (7)$$

In order to further reduce the complexity of the linearizer, the idea is to estimate in offline the FW sub-model with a large number of coefficients to describe the main inverse PA characteristics,

while the MP structure will be minimized by reducing as much as possible the orders P_a and M_a to operate in real time. The FW system will then be fixed regardless of the application and only the MP sub-model will be updated to take into account variations and changes in the PA environment such as the waveform, temperature, bias voltage, and/or aging.

Identification algorithm

As mentioned previously, the MP model will be estimated in real time during the use of the PA. The FW model must be estimated beforehand. One of the fundamental characteristics in the FW system is its cascaded structure [32, 34, 39, 40], and here the focus will be on the unmeasured intermediate signals $v(n)$ and $w(n)$, required for the estimation process.

From Eqs. (1) and (2), we can write the FW output by separating the first term such as

$$v(n) = c_1 \left(g_0 x(n) - \sum_{m=1}^M b_m v(n-m) \right) + \sum_{p=2}^P c_p w(n)^p. \tag{8}$$

Noted that the gains g_0 and c_1 are correlated and to avoid the overparametrization problem [40], c_1 is set to one and only g_0 is estimated. Thus, for parameters estimation, the FW block can be expressed in linear regression system:

$$v(n) = g_0 x(n) - \sum_{m=1}^M b_m v(n-m) + \sum_{p=2}^P c_p w(n)^p = \underline{\varphi}(n)^T \cdot \hat{\underline{\theta}}_{FW}, \tag{9}$$

where $\underline{\varphi}_n$ is the regressor vector and $\hat{\underline{\theta}}_{FW}$ is the vector of coefficients to be estimated:

$$\hat{\underline{\theta}}_{FW} = [g_0 \quad b_1 \cdots b_M \quad c_2 \cdots c_P]^T \tag{10}$$

$$\underline{\varphi}(n) = [x(n) \quad -v(n-1) \cdots -v(n-M) \quad w(n)^2 \cdots w(n)^P]^T.$$

Noted that in the linearization scheme, the aim is to modelize the inverse PA characteristic. Thus, $v(n)$ is replaced by the PA input, $x(n)$ by the normalized output $\hat{y}(n)$, $v(n-m)$ and $w(n)$ by their simulation during the identification process. The parameter vector $\hat{\underline{\theta}}_{FW}$ is obtained by minimizing the quadratic criterion J based on N measured samples such as

$$J = \sum_{n=1}^N \varepsilon(n)^2, \tag{11}$$

where $\varepsilon(n)$ is the complex-envelope error between measured input $x'(n)$ and its estimation $\hat{x}'(n)$.

Once the FW block has been identified, its coefficients are maintained constant during operation. The aim is now to find an MP model that describes the modeling error, remaining after the FW block, as accurately as possible. We propose then to use the recursive weighted least squares (RWLS) algorithm for the real-time identification. The RWLS algorithm [41] is a recursive form of the ordinary LS method [42], which is performed sample by sample to identify the parameters that are subject to change to maintain the tracking ability. The main principle of the RWLS technique is to

introduce a forgetting factor λ that gives greater importance to the recent measurements [43]. The parameter vector $\hat{\underline{\theta}}_{MP}(n)$ is updated at each iteration n such as

$$\hat{\underline{\theta}}_{MP}(n) = \hat{\underline{\theta}}_{MP}(n-1) + K(n) (x'(n) - \hat{x}'(n)), \tag{12}$$

where $K(n)$ is the gain matrix depending on the coefficients covariance matrix $C(n)$, such as

$$K(n) = \frac{C(n-1)\underline{\phi}^*(n)}{\lambda + \underline{\phi}^H(n)C(n-1)\underline{\phi}(n)}, \tag{13}$$

$$C(n) = \lambda^{-1} (C(n-1) - K(n)\underline{\phi}^*(n)C(n-1)), \tag{14}$$

where $\underline{\phi}(n)$ is the MP regressor vector defined in Eq. (5), $(\cdot)^*$ and $(\cdot)^H$ represent, respectively, the conjugate operation and the transposition-conjugate transform.

Experimental results

The proposed structure has been used for the linearization of a 75 W UHF/VHF PA designed by Telerad Society for aeronautical communications. The test bench used in this study is shown in Fig. 2. The PA input is a Quadrature Phase Shift Keying modulated signal with 16.8 kHz bandwidth at the carrier frequency of 127.5 MHz. The output is recovered via a directional coupler and then digitally converted by a fast ADC converter. The input and output signals are synchronized using a cross-correlation technique.

For the measurements, different carrier frequencies, different PA bias voltages, and different operating temperatures were tested. In our targeted airborne VHF applications, the VDL2 standard imposes strong constraints on the ACPR values. The out-of-band spurious emissions are specified by the first- and second-order ACPR such as

- $ACPR_{L1}, ACPR_{U1} < -65$ dB
- $ACPR_{L2}, ACPR_{U2} < -75$ dB

The first adjacent band is located at 25 kHz from the main band and with 16.8 kHz of width ($ACPR_{L1}$ and $ACPR_{U1}$) when the second adjacent band is located at 50 kHz from the main band and with 25 kHz of width ($ACPR_{L2}$ and $ACPR_{U2}$). L and U denote the lower and upper bands, respectively, which are located in the left and right of the main band.

The first step is to determine the minimum structure of the MP model needed to guarantee the specifications. Then, we look for the optimal structure of the FWMP model with a minimum number of coefficients.

Table 1 gives the obtained ACPR values for different structures of MP and FW blocks. For better readability and unlike the values shown in bold italic, which shows the respect for the standard, the other values in plain format indicate that the specifications are not reached. The analysis of these results shows that it is impossible to reduce the number of coefficients in the MP block beyond 8 (see the three last lines). The introduction of the FW block improves the results on the L2 and U2 bands, for which the constraints are difficult to meet. Although a reduced two-coefficient FW block allows the respect of the specification (model in line 3), for a safety margin, we used the FWMP model with an MP block of eight coefficients and an FW block of three coefficients (model in line 4).

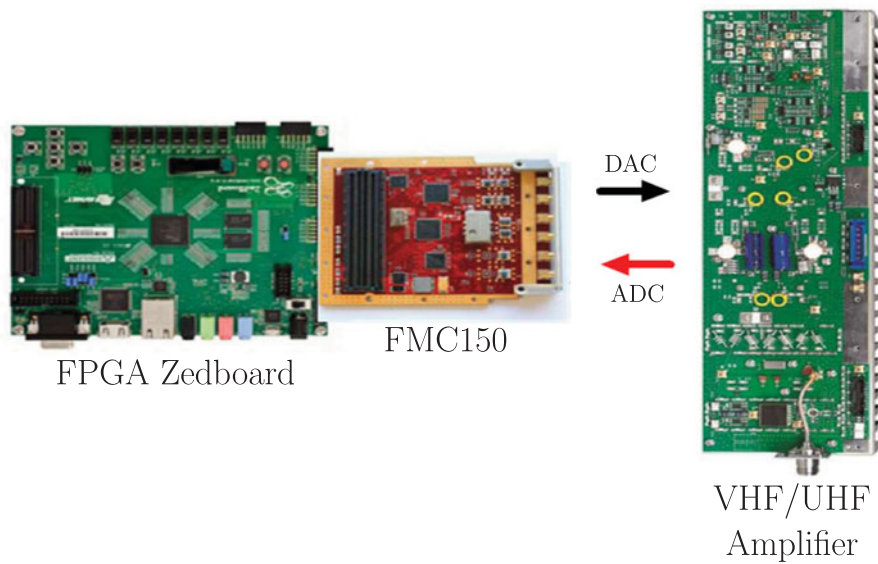


Figure 2. Amplifier to be linearized and digital boards.

Table 1. Optimal MP and FWMP structures

Number of MP	Coefficients FW	$ACPR_{L_2} < -75$ dB	$ACPR_{L_1} < -65$ dB	$ACPR_{U_1} < -65$ dB	$ACPR_{U_2} < -75$ dB
9	0	-79.01	-78.75	-78.51	-79.20
8	0	-72.20	-74.33	-74.56	-72.69
8	2	-76.89	-77.41	-77.03	-77.59
8	3	-79.15	-78.27	-77.73	-80.13
8	4	-79.82	-78.56	-77.94	-80.88
7	2	-67.56	-70.74	-70.97	-68.11
7	3	-68.20	-71.22	-71.38	-68.80
7	4	-67.57	-70.68	-70.81	-68.25

Considering the optimized FWMP structure with 11 coefficients ($P = 3$, $M = 0$, $P_a = 8$, and $M_a = 1$) with 3 fixed coefficients for FW block and 8 estimated coefficients for the MP block, the ACPR results without and with DPD (in offline and online versions), using a modulated signal transposed on a carrier frequency of 127.5 MHz, are presented in Table 2 for a symbol rate of 10 kS/s. This structure is compared to an MP model with nine coefficients ($P_a = 9$ and $M_a = 1$).

Table 2 is decomposed into three parts: the first one gives the results without DPD, followed by the results of the offline linearization with the MP models alone and the proposed model. The last part shows the results of both models in the online version.

Here, offline DPD consists of applying a static predistorter, estimated from measurements at 127.5 MHz. The estimation of the offline DPD models (MP and FWMP) is carried out by the least squares algorithm [32, 35]. There is no update of the DPD coefficients in this case. The online DPD architecture is the one described in Fig. 1, using the recursive algorithm described in Eqs. (12)–(14).

From this table, it can be seen that, contrary to the case without DPD, the offline DPD functions based on the MP model (9 coefficients) and the FWMP model allow to achieve the specifications (values in bold italic). However, switching to the online mode

deteriorates the performance of the MP and FWMP model on the U_2 and L_2 side bands, but the DPD based on the proposed FWMP structure maintains the respect of the specifications. Also, note that only eight tunable coefficients are updated in the case of the FWMP model.

Output spectra with and without DPD based on the two models MP and FWMP are shown in Fig. 3. The real-time adjustment of the DPD parameters allows an improvement of about 40 dB in the lower and upper first side bands.

Table 3 presents a comparison of the estimated vector $\hat{\theta}_{MP}$ for both MP and FWMP models, resulting from the two versions of identifications (offline and online). This allows to see how the parameters of the MP block evolve between the two versions for each model.

We can see from Table 3 that the FWMP model obtained in offline version is very close to that obtained in real time with the RLWS algorithm. This is not the case for the MP model where the values of the coefficients are different. This result is predictable because the MP structure is a black-box model without any physical significance, contrary to the FWMP model where FW block is close to the behavior of PA [38]. In the case of the FWMP model, use of the FW block helps to make the variations in the MP block less fluctuating.

Table 2. ACPR without and with DPD

Model	ACPR _{L2} < -75 dB	ACPR _{L1} < -65 dB	ACPR _{U1} < -65 dB	ACPR _{U2} < -75 dB
Without DPD	-54.11	-37.65	-35.68	-52.59
<i>Offline DPD</i>				
MP (9 coefficient)	-79.01	-78.75	-78.51	-79.20
FW fixed + MP (3 coefficient) + (8 coefficient)	-79.15	-78.27	-77.73	-80.13
<i>Online DPD</i>				
MP (9 coefficient)	-72.42	-73.96	-73.79	-71.30
FW fixed + MP (3 coefficient) + (8 coefficient)	-75.87	-77.37	-78.15	-76.79

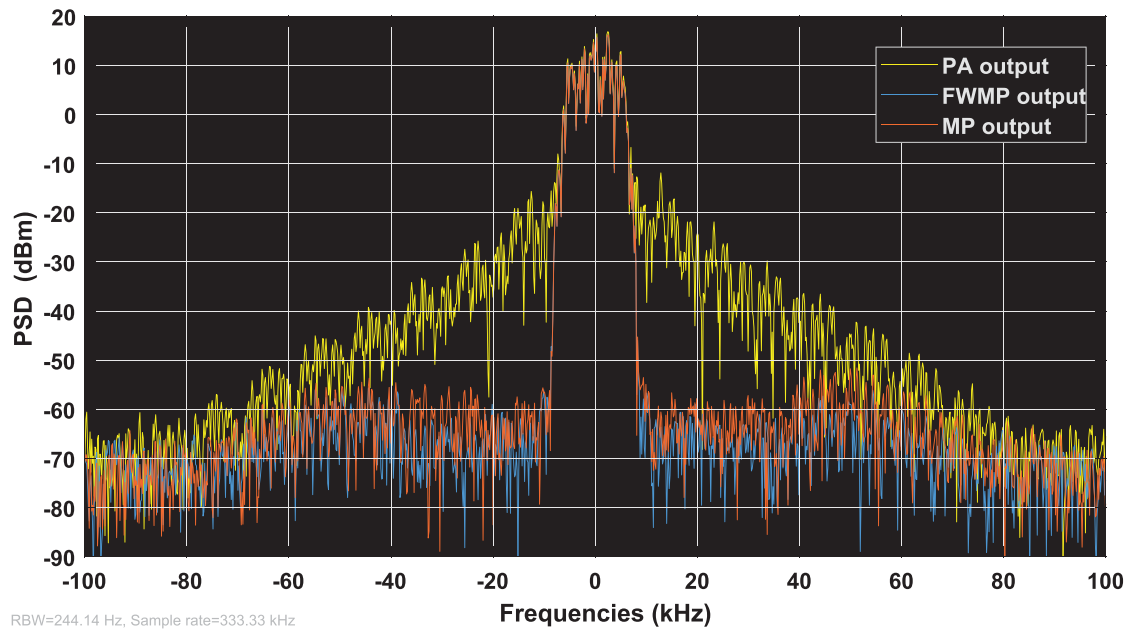


Figure 3. Output spectra with and without DPD.

In general case, the complexity of the RLS algorithm is dominated by the complexity of updating the gain matrix $K(n)$ in Eqs. (13) and (14), which requires a computational load by $\mathcal{O}(N^2)$ operations per iteration, where N is the number of coefficients. The other steps of the algorithm have a complexity at most linear in $\mathcal{O}(N)$.

In the time domain, the AM/AM curves with and without linearization using the adaptive DPD, with a fixed FW block and only the MP block coefficients to be updated, are presented in Fig. 4. We can see that the proposed structure improves the linearity of the communication system.

In order to test the robustness of the proposed model, we study the effect of the temperature changes at 26, 31, and 36°C by switching the PA with the previously identified models at each temperature. Figure 5 shows the convergence of the coefficients during operation, while Fig. 6 gives the linearization error between the PA input $x(n)$ and the normalized PA output $\hat{y}(n)$. Note that the used FW structure is the one obtained at 36°C.

The obtained results (Fig. 5) show that the algorithm based on the FWMP model adapts to temperature changes. Also, we can see from the comparison between the input and the linearized output (Fig. 6) that the difference is small, which means that during temperature changes, the system is able to adapt in a robust way. In

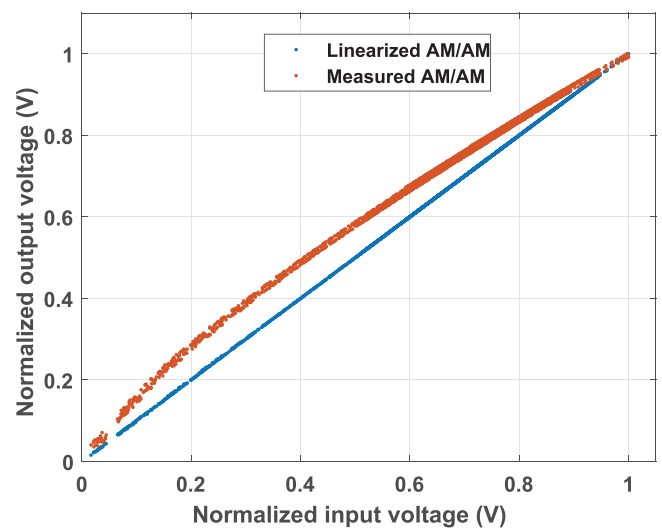


Figure 4. AM/AM curves with and without linearization.

practice, the algorithm converges after the temperature change in about 1 ms.

Table 3. Evolution of $\hat{\theta}_{-MP}$ for MP and FWMP models (in offline and online versions)

Model coefficient	FW fixed (3 coefficients) + MP (8 coefficients)		MP (9 coefficients)	
	Offline	Online	Offline	Online
a_{00}	$0.0108 + 0.0023j$	$0.0109 + 0.0024j$	$0.0052 - 0.0034j$	$-0.0010 + 0.0010j$
a_{10}	$-0.0227 - 0.0395j$	$-0.0234 - 0.0403j$	$0.0143 + 0.0189j$	$0.0192 - 0.0172j$
a_{20}	$0.1867 + 0.2604j$	$0.1881 + 0.2615j$	$-0.1675 - 0.1904j$	$-0.1410 + 0.1206j$
a_{30}	$-0.7109 - 0.8735j$	$-0.7038 - 0.8616j$	$1.1206 + 1.0401j$	$0.5685 - 0.4611j$
a_{40}	$1.4587 + 1.6408j$	$1.4224 + 1.5853j$	$-3.6533 - 3.0061j$	$-1.3752 + 1.0626j$
a_{50}	$-1.6680 - 1.7483j$	$-1.6043 - 1.6490j$	$6.5822 + 4.9654j$	$2.0506 - 1.5174j$
a_{60}	$1.0014 + 0.9876j$	$0.9520 + 0.9059j$	$-6.7278 - 4.7317j$	$-1.8469 + 1.3154j$
a_{70}	$-0.2460 - 0.2299j$	$-0.2317 - 0.2041j$	$3.6611 + 2.4234j$	$0.9219 - 0.6346j$
a_{80}			$-0.8248 - 0.5170j$	$-0.1958 + 0.1307j$
	$\times 10^2$	$\times 10^2$	$\times 10^2$	$\times 10^4$

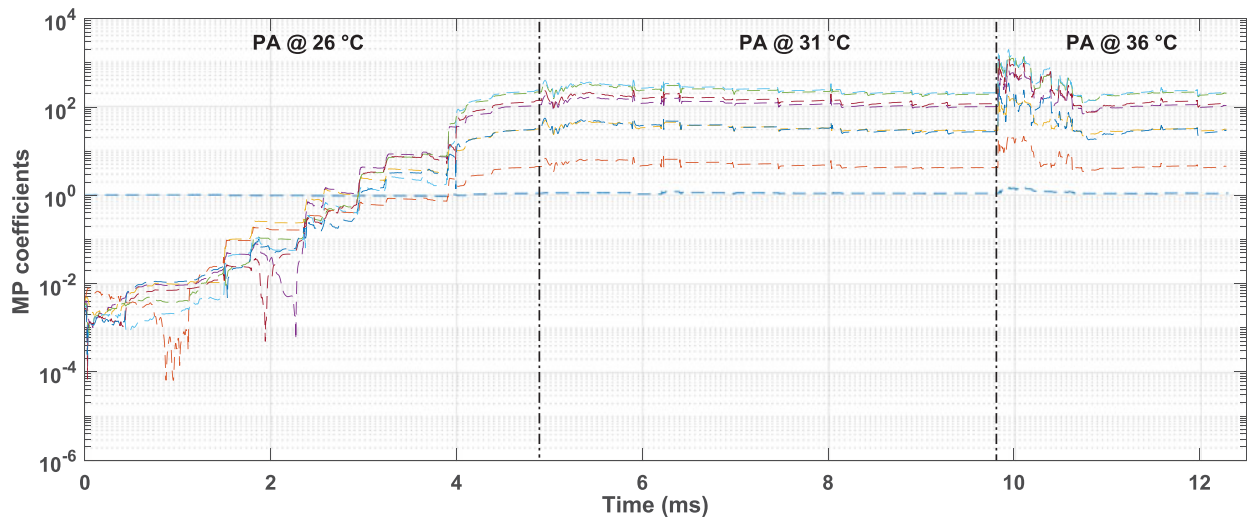


Figure 5. Variation of MP coefficients versus temperature changes.

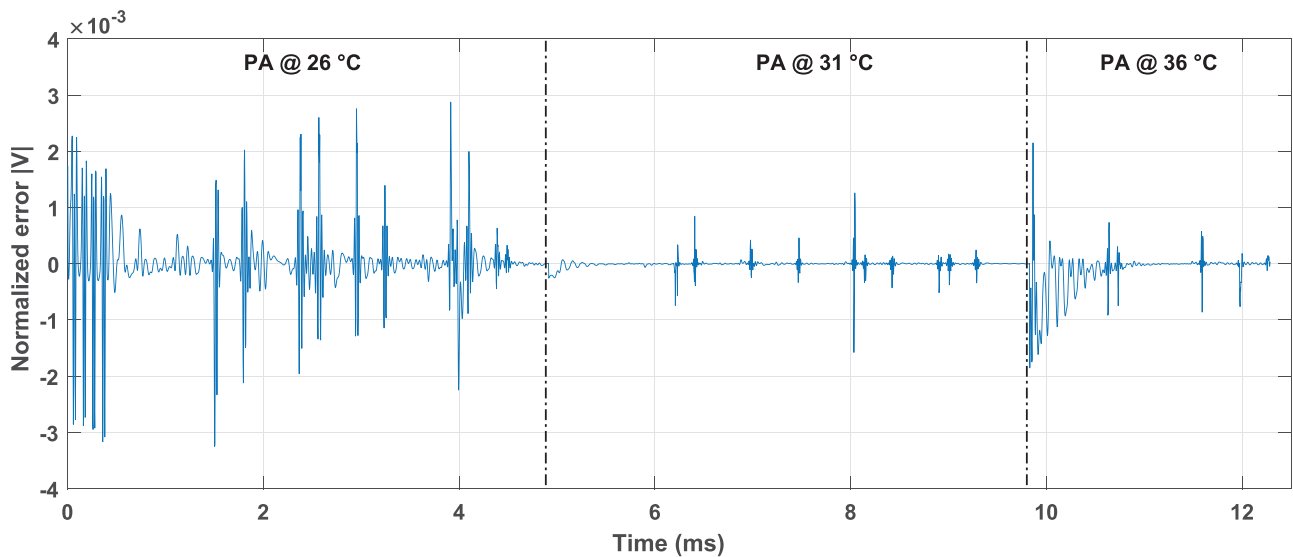


Figure 6. Linearization error versus temperature changes.

The value of the forgetting factor $\lambda \in]0, 1]$ has a significant influence on the performance of the algorithm. When it is close to unity, the online algorithm achieves good robustness, but the convergence becomes slower, like the Gradient algorithm. A smaller value improves the speed convergence but it increases the probability of being unstable. In this case, fluctuations appear on the estimates because the new measured samples are more weighted in the algorithm.

In our case, we choose $\lambda = 0.95$, which achieves a good trade-off between the stability and the tracking ability, with a time convergence of about 1 ms.

Conclusion

A new DPD based on an FW model has been proposed in this study. In this approach, we used a reduced complexity structure with a real-time tunable MP block. Adjustment of the MP block allows tracking of changes in the nonlinear behavior when the RF PA is operating. The RLWS algorithm is introduced to design and estimate the complex predistortion with memory in real time. Also, the optimization process includes a step to characterize the minimum orders of the model to insure convergence, stability and reduced number of calculation during estimation.

To meet the industrial requirements in terms of high-speed processing and complexity of implementation, the main FW part of the DPD is maintained constant during operation, and only the MP block is adapted. This speeds up the algorithm's convergence and decreases the execution time.

The effectiveness of this approach is demonstrated through studies in aeronautical applications using aircraft-ground signals. The results show that the proposed predistorter is able to be more accurate in the characterization of the inverse nonlinear PA, even if its behavior changes according to the operating conditions. Despite the strong criteria, in terms of ACPR values, in the aeronautical domain, the FWMP-based system shows a good ACPR reduction illustrated by an improvement of about 40 dB in spectral regrowths.

Acknowledgements. Research reported in this publication is part of the APOGEES project supported by BPI France, region Occitanie and region Nouvelle Aquitaine. APOGEES project has been labeled by pole Aerospace Valley, pole I&R, and pole Alpha-RLH in the framework of the French FUI22 research program.

Competing interests. The authors report no conflict of interest.

References

1. **Budinger J** (2005) Technology Assessment for the Future Aeronautical Communications System. NASA/CR-2005-213587, Reston, Virginia: ITT industries, NASA.
2. **Zaruba R** (2015) Air/ground data communication radios for future ATM. In *2015 IEEE/AIAA 34th Digital Avionics Systems Conference (DASC)*, Prague, Czech Republic, pp. 2F4-1–2F4-10.
3. **Aitchison CS, Mbabele M, Moazzam MR, Budimir D and Ali F** (2001) Improvement of third-order intermodulation product of RF and microwave amplifiers by injection. *IEEE Transactions on Microwave Theory and Techniques* **49**, 1148–1154.
4. **Carvalho N and Pedro J** (1999) Multi-tone intermodulation distortion performance of 3rd order microwave circuits. In *1999 IEEE MTT-S International Microwave Symposium Digest*, Anaheim, CA, USA, Volume 2, 763–766.
5. **Boulejfen N, Harguem A, Hammi O, Ghannouchi FM and Gharsallah A** (2010) Analytical prediction of spectral regrowth and correlated and uncorrelated distortion in multicarrier wireless transmitters exhibiting memory effects. *IET Microwaves, Antennas & Propagation* **4**, 685–696.
6. **McKinley MD, Remley KA, Myslinski M and Kenney JS** (2004) EVM calculation for broadband modulated signals. In *64th ARFTG Microwave Measurement Conference Digest*, Orlando, FL, USA, pp. 45–52.
7. **Pedro JC and Maas SA** (2005) A comparative overview of microwave and wireless power amplifier behavioral modeling approaches. *IEEE Transactions on Microwave Theory and Techniques* **53**, 1150–1163.
8. **Kim J and Konstantinou K** (2001) Digital predistortion of wideband signals based on power amplifier model with memory. *Electronics Letters* **37**, 1417–1418.
9. **Tehrani A, Cao H, Afsardoost S, Eriksson T, Isaksson M and Fager C** (2010) A comparative analysis of the complexity/accuracy tradeoff in power amplifier behavioral models. *IEEE Transactions on Microwave Theory and Techniques* **58**, 1510–1520.
10. **Wood J and Bertran E** (2013) Special issue on power amplifier linearization. *International Journal of Microwave and Wireless Technologies* **5**, 101–102.
11. **Rawat M and Ghannouchi F** (2012) Distributed spatiotemporal neural network for nonlinear dynamic transmitter modeling and adaptive digital predistortion. *IEEE Transactions on Instrumentation and Measurement* **61**, 595–608.
12. **Tabatabai F and Al-Raweshidy HS** (2007) Feedforward linearization technique for reducing nonlinearity in semiconductor optical amplifier. *Journal of Lightwave Technology* **25**, 2667–2674.
13. **Zhao G, Ghannouchi FM, Beauregard F and Kouki AB** (1996) Digital implementations of adaptive feedforward amplifier linearization techniques. In *1996 IEEE MTT-S International Microwave Symposium Digest*, San Francisco, CA, USA, pp. 543–546.
14. **Stapleton SP and Costescu FC** (1992) An adaptive predistorter for a power amplifier based on adjacent channel emissions (mobile communications). *IEEE Transactions on Vehicular Technology* **41**, 49–56.
15. **Chen S** (2011) An efficient predistorter design for compensating nonlinear memory high power amplifiers. *IEEE Transactions on Broadcasting* **57**, 856–865.
16. **Wood J** (2017) System-level design considerations for digital predistortion of wireless base station transmitters. *IEEE Transactions on Microwave Theory and Techniques* **65**, 1880–1890.
17. **Bacque L, Nanfack-Nkondem G, Bouysse P, Neveux G, Nebus J, Rebernak W, Lapierre L, Barataud D and Quéré R** (2009) Implementation of dynamic bias and digital predistortion to enhance efficiency and linearity in a 100 W RF amplifier with OFDM signal. *International Journal of Microwave and Wireless Technologies* **1**, 261–268.
18. **Woo W and Kenney JS** (2005) A predistortion linearization system for high power amplifiers with low frequency envelope memory effects. In *2005 IEEE MTT-S International Microwave Symposium Digest*, Long Beach, CA, USA.
19. **Kim W-J, Stapleton SP, Kim JH and Edelman C** (2005) Digital predistortion linearizes wireless power amplifiers. *IEEE Microwave Magazine* **6**, 54–61.
20. **Gilbert Pinal PL** (2007) *Multi Look-Up Table Digital Predistortion for RF Power Amplifier Linearization*. PhD Thesis, Barcelona, Spain: Polytechnic University of Catalonia.
21. **Bachir S, Nicusor CE and Duvanaud C** (2011) Linearization of RF power amplifiers using adaptive Kalman filtering algorithm. *Journal of Circuits, Systems, and Computers* **20**, 1001–1018.
22. **Vaskovic M** (2014) *Compensation of Nonlinear Distortion in RF Amplifiers for Mobile Communications*. PhD Thesis, London, England: University of Westminster.
23. **Liu T, Boumaiza S and Ghannouchi FM** (2006) Augmented Hammerstein predistorter for linearization of broad-band wireless transmitters. *IEEE Transactions on Microwave Theory and Techniques* **54**, 1340–1349.
24. **Hamoud HE, Reveyrand T, Mons S and Ngoya E** (2018) A comparative overview of digital predistortion behavioral modeling for multi-standards applications. *International Workshop on Integrated Nonlinear Microwave and Millimetre-wave Circuits (INMMIC)*, Brive La Gaillarde, France, pp. 1–3.

25. **Schetzen M** (2006) *The Volterra and Wiener Theories of Nonlinear Systems*. Melbourne, FL, USA: Krieger Publishing Co.
26. **Eun C and Powers EJ** (1997) A new Volterra predistorter based on the indirect learning architecture. *IEEE Transactions on Signal Processing* **45**, 223–227.
27. **Ngoya E, Quindroit C and Nebus JM** (2009) On the continuous-time model for nonlinear-memory modeling of RF power amplifiers. *IEEE Transactions on Microwave Theory and Techniques* **57**, 3278–3292.
28. **Alizadeh M, Händel P and Rönnow D** (2019) Behavioral modeling and digital pre-distortion techniques for RF PAs in a 3×3 MIMO system. *International Journal of Microwave and Wireless Technologies* **11**, 989–999.
29. **Messaoudi N, Fares MC, Boumaiza S and Wood J** (2008) Complexity reduced odd-order memory polynomial pre-distorter for 400-watt multi-carrier Doherty amplifier linearization. In *2008 IEEE MTT-S International Microwave Symposium Digest*, pp. 419–422.
30. **Morgan DR, Ma Z, Kim J, Zierdt MGZ and Pastalan J** (2006) A generalized memory polynomial model for digital predistortion of RF power amplifiers. *IEEE Transactions on Signal Processing* **54**, 3852–3860.
31. **Afsardoost S, Eriksson T and Fager C** (2012) Digital predistortion using a vector-switched model. *IEEE Transactions on Microwave Theory and Techniques* **60**, 1166–1174.
32. **Wang S** (2018) *Study on Complexity Reduction of Digital Predistortion for Power Amplifier Linearization*, PhD Thesis, Paris, France: ESIEE Paris Est.
33. **Braithwaite RN and Carichner S** (2009) An improved Doherty amplifier using cascaded digital predistortion and digital gate voltage enhancement. *IEEE Transactions on Microwave Theory and Techniques* **57**, 3118–3126.
34. **Wang S, Abi Hussein M, Venard O and Baudoin G** (2018) Optimal sizing of two-stage cascaded sparse memory polynomial model for high power amplifiers linearization. *IEEE Transactions on Microwave Theory and Techniques* **66**, 3958–3965.
35. **Bouazza THC, Bachir S and Duvanaud C** (2019) Behavioral blocks model for complexity-reduced modeling of RF power amplifiers. In *2019 IEEE International Symposium on Circuits and Systems (ISCAS)*, Sapporo, Japan, 26–29.
36. **Vu V-K and Tran V-N** (2020) Adaptive digital predistortion of RF power amplifiers based on memory polynomial model and indirect learning architecture. In *2020 International Conference Engineering and Telecommunication (En&T)*, Dolgoprudny, Russia, pp. 7974–7978.
37. **Yu C, Tang Q and Liu Y** (2018) A novel indirect learning digital predistortion architecture only with in-phase component. In *2018 Asia-Pacific Microwave Conference (APMC)*, Kyoto, Japan, pp. 995–997.
38. **Bouazza THC** (2021) *Modélisation et linéarisation des amplificateurs de radiocommunications dans un contexte de reconfigurabilité*, PhD Thesis, France: University of Poitiers.
39. **Narendra K and Gallman P** (1966) An iterative method for the identification of nonlinear systems using a Hammerstein model. *IEEE Transactions on Automatic Control* **11**, 546–550.
40. **Zhu A, Pedro JC and Cunha TR** (2007) Pruning the Volterra series for behavioral modeling of power amplifiers using physical knowledge. *IEEE Transactions on Microwave Theory and Techniques* **55**, 813–821.
41. **Haykin S** (2002) *Adaptive filter theory*. New Jersey: Prentice Hall.
42. **Zhou GT and Raich R** (2004) Spectral analysis of polynomial nonlinearity with applications to RF power amplifiers. *EURASIP Journal on Advances in Signal Processing* **2004**, 1831–1840.
43. **Li Y and Zhang X** (2011) A modified RLS algorithm for identification of power amplifier nonlinear model. In *Proceedings of 2011 International Conference on Computer Science and Network Technology*, Volume 4, Harbin, China, pp. 2307–2310.



Tayeb H. C. Bouazza received his B.Sc. and M.Sc. in Electronics and Telecommunications from the University of Saïda, Algeria, in 2011 and 2013, respectively. He joined the Department of Smart Networks and Systems, XLIM Laboratory and the University of Poitiers, France, where he received his Ph.D. degree in Electronics, Microelectronics, Nanoelectronics, and Microwaves in 2021. His current research interests are in modeling nonlinear systems, signal processing, and wireless communication. ORCID: <https://orcid.org/0000-0003-3873-0087>



Smil Bachir received both B.Sc. and M.Sc. in Signal Theory from Polytechnic School of Algeria in 1997. He joined the scientific department of Leroy Somer Society and the University of Poitiers in France, where he received his Ph.D. degree in Automatic and Electrical Engineering in 2002 and the Habilitation Degree (HDR) in 2015. He is presently an Associate Professor at the University of Poitiers and a researcher at XLIM Laboratory with the Department of Smart Networks and Systems. His research interests include signal processing, nonlinear systems parameter identification, and wireless system.



Matthieu Pastore was graduated from the Supélec College in 2010. He received the master's degree from IETR in 2010. His end-term projects concerned reconfigurable software radio architectures (implementation of an HDCRAM model on GNURadio and USRP). From 2011 to 2012, he was with Zodiac DataSystem, where he was involved in the design and implementation on FPGA target of high data rate satellite receiver algorithms. He has been with Telerad Company since 2012. He is in charge of the design and implementation of various DSP algorithms for air traffic control VHF receivers and transmitters: simultaneous call detection, high dynamic reception, audio and RF quality measures, and linearization.



Claude Duvanaud received his Ph.D. in Electronics and Communication Engineering from the University of Limoges, France, in 1993 and the Habilitation Degree (HDR) from the University of Poitiers in 2003. He currently is an Associate Professor at the University of Poitiers and XLIM Laboratory, France. His research interests include modeling, simulation, and design of nonlinear Power Amplifiers and Communication systems.